Evolutions of Competition of Multiple-Spin-Exchange Interactions and Structure in Submonolayer Solid ^{3}He Film Adsorbed on Grafoil

Masashi Morishita

Institute of Physics, University of Tsukuba, Tsukuba, Ibaraki 305-8571, Japan

Takeo Takagi

Department of Applied Physics, Fukui University, Fukui 910-8507, Japan
(Received 11 July 2001; published 15 October 2001)

For ^{3}He submonolayer solid adsorbed on Grafoil, the evolutions of the adsorption structure and of the competition of multiple-spin-exchange interactions with increasing areal density are discussed. The discrepancy of the heat-capacity exponent from the normal value, -2, is considered to show the strength of the competition. We give various discussions to explain the density dependence of the competition, the sudden change of the exchange frequency, and other observations. There we propose the structural phase diagram constructed from the simulations and the possible zero-point vacancies.

Much attention has been attracted to the low-dimensional frustrated quantum spin systems. ^{3}He solid film physisorbed on a graphite surface is one of the most ideal two-dimensional (2D) quantum spin systems [1]. The facts that the magnetism is dominated by the multiple spin exchange (MSE) interactions and the frustration is strengthened by the MSE competition are striking features of this system [1–3]. The magnetism changes as ferromagnetic (FM)-antiferromagnetic (AFM)-FM in the submonolayer [4] and as AFM-FM in the second layer [5] with increasing areal density. These evolutions have been understood qualitatively with the different density dependencies of each MSE [2] and with the suppression of the two-spin exchange by the corrugation of the adsorption potential at the low-density region of the submonolayer [4]. However, the detailed mechanisms are not clearly understood which causes the sudden change from AFM to FM within the rather narrow density regime followed by the ferromagnetic peak of the exchange frequency J [4–6]. That would be mainly due to the lack of knowledge of the adsorption structures. In this Letter we give discussions about the evolutions of the adsorption structure and of the MSE competition with increasing density, and examine them by comparison with some experimental observations.

The frustration parameter $\zeta = -(J_4 - 2J_5)/(J_2 - 2J_3)$ introduced by Roger *et al.* [3] is a measure of the strength of the MSE competition or the importance of higher order MSEs. Here J_n is the n-spin exchange frequency. While the ζ value for the second layer ^{3}He has been obtained by them, no ζ value for the submonolayer has yet been obtained. On the other hand, anomalous temperature (T) dependence of the heat capacity (C), $C \propto T^\alpha (\alpha \approx -1)$, is observed in wide temperature and density ranges, instead of $C \propto T^{-2}$ behavior expected for any localized spin system in the high temperature limit. The experimental details are described in Ref. [7]. There the anomalous T dependence of C is attributed to the strong MSE competition and some supporting evidence is discussed. Here

we further advance the thought and adopt the model that the discrepancy of α from the expected normal value, -2, can be considered as a frustration parameter showing the strength of the MSE competition. According to this model the behavior of α shown in Fig. 1 indicates that the MSE competition is strong at almost the whole density range. One of the reasons for the strong competition is the strong adsorption potential, which restricts the exchange tunnel paths in 2D space more strictly and suppresses the MSEs, especially the fewer body MSEs. The strong corrugation of the adsorption potential, whose amplitude is about 40 K in the first layer [8], increases the exchange barrier height and suppresses the MSEs. That must also affect the MSE competition.

In Fig. 1 several distinctive structures of α can be seen: (*A*) a gradual increase at $\rho \lesssim 6.5$ nm^{-2}, (*B*) a steep drop near $\rho = 7.5$ nm^{-2}, and (*C*) a spike around $\rho = 8.5$ nm^{-2}. In the following we examine these features of α as the change of the MSE competition discussing the evolution of adsorption structure.
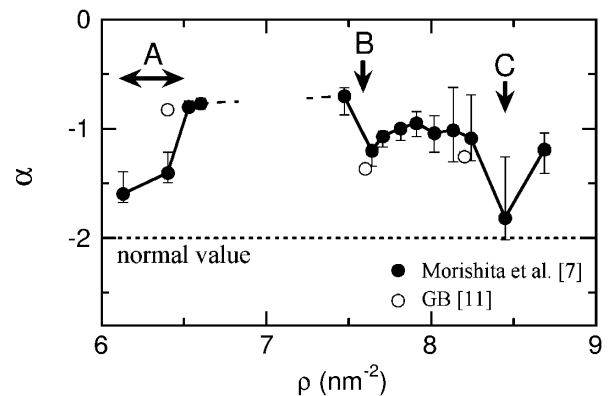

FIG. 1. The exponents (α) of heat capacities (C) of submonolayer ^{3}He films as functions of areal density (after Ref. [7]). Some distinctive structures can be seen where marked by arrows.

The gradual increase of α at $\rho \lesssim 6.5$ nm^{-2} (A) can be thought to result from the decrease of the zero-point vacancies. Slightly below the density of the $\sqrt{3} \times \sqrt{3}$ phase (6.4 nm^{-2}) vacancies are expected to exist [9], although no direct evidence has been observed until now. In the heat-capacity measurements of 6.1 and 6.4 nm^{-2} ^{3}He films no heat-capacity contribution from the fluid phase is observed, but the bump structures around 20 mK are observed [7]. The observed bump height of about 0.1 mJ/K is too small for the formation of the "thermal" vacancy. For example, at 6.1 nm^{-2} the heat-capacity peak of the vacancy formation should be about 10 mJ/K. Even down to about 0.1 mK, which is the order of the exchange frequency, no anomalous heat-capacity behavior suggesting the formation of thermal vacancies has been observed. So, the possible vacancy is the ground-state (zero-point) vacancy practically. The observed heat-capacity bumps are likely due to the spin polaron effects induced by the zero-point vacancy [7,10]. The vacancy must facilitate the spin exchange, especially two- or three-spin exchanges which are suppressed by hard-core repulsion without vacancy. So the existence of vacancy should weaken the MSE competition.

In the density region above 6.4 nm^{-2} the adsorption structures have not been confirmed experimentally. Greywall and Busch (GB) have proposed a phase diagram assuming some registered solid phases and the incommensurate (IC) phase [6,11]. Lauter *et al.* have proposed the existence of the domain wall phase [12]. However, these predictions failed to explain the sudden FM peak of J. Here we seek a more reliable phase diagram based on simulations. Unfortunately it is difficult to make a comprehensive study of all structures. So we obtain the structural phase diagram based on the calculations of adsorption energy in several limited but plausible structures and examine that by comparing with experimental observations.

One candidate of plausible structure is the domain wall structure. It must evolve from the striped one to the honeycomb one with the increase of density. Within the honeycomb domain wall (HDW) structures the $(3n + 1) \times (3n + 1)$ (n, integer) series is expected to be more stable than other series. For example, the 10×10 and 7×7 HDW structures have the areal density of 7.07 nm^{-2} and 7.41 nm^{-2}, respectively. Between and below these areal densities the adsorbed system is described by the network of similar heavy domain walls.

We propose other honeycomb structures schematically shown in Fig. 2. The $12/36 = 1/3$ structure is the $\sqrt{3} \times \sqrt{3}$ phase. We propose that when atoms are added the honeycomb structures of ^{3}He atoms indicated by thick lines survive. The density increases only inside each hexagonal cage as shown in Fig. 2. The $12/36 = 1/3$, $13/36$, $14/36$, and $15/36$ phases correspond to the density of 6.37, 6.90, 7.43, and 7.96 nm^{-2}, respectively. In the intermediate region of these densities two of these phases are supposed to coexist. We call these structures "honeycomb cage" structures for convenience. We can imagine other sizes of
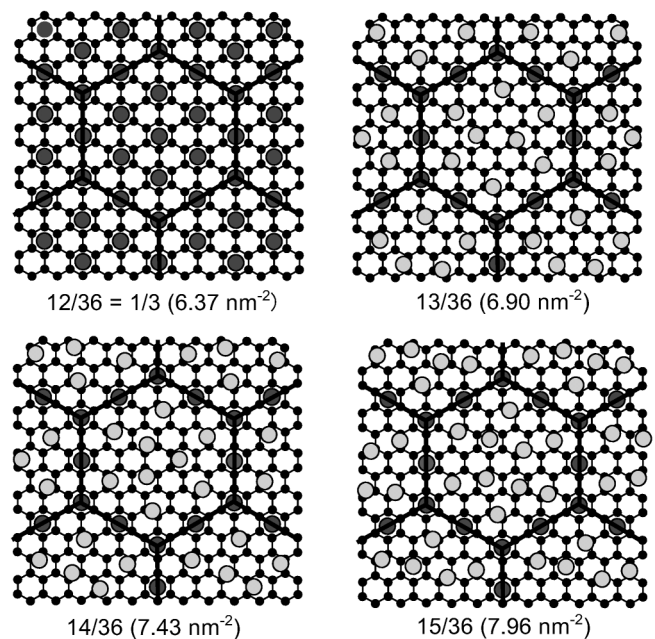

12/36 = 1/3 (6.37 nm^{-2})   13/36 (6.90 nm^{-2})

14/36 (7.43 nm^{-2})   15/36 (7.96 nm^{-2})

FIG. 2.   The proposed "honeycomb cage" adsorption structures of the submonolayer ^{3}He films on graphite. The dots show the positions of carbon atoms, and the small honeycombs show the lattice of graphite. The grey circles are ^{3}He atoms.

honeycomb cage structure, but they seem unstable and do not appear.

We calculated the energy of adsorbed ^{3}He atoms on graphite for these structures by the path integral Monte Carlo simulation under the periodic boundary condition. The details of the method and the results of the calculation will be described elsewhere. The calculated adsorption energies per atom are shown in Fig. 3. Although the cage structures have never been observed in any adsorbed system, our calculations show that they are more stable than the HDW at the higher density region.

Now let us consider the evolution of structure. When the density is increased from the $\sqrt{3} \times \sqrt{3}$ phase, the
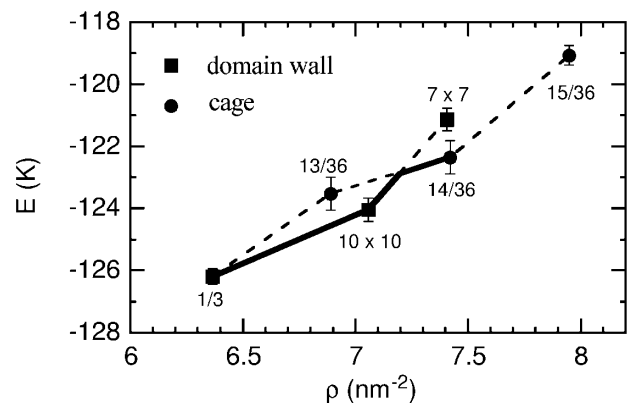

FIG. 3.   The adsorption energies per ^{3}He atom for the honeycomb domain wall structures (squares) and honeycomb cage structures (circles) calculated by path integral Monte Carlo simulations.

striped domain wall structure appears and then evolves to the HDW structure. The cage structures then appear. Here the HDW structure (10×10) and the cage structure (14/36) seem not to coexist because of the large boundary energy. So a second-order structural phase transition should occur at $\rho \approx 7.2$ nm^{-2}. The energy evolves as shown by the thick line in Fig. 3. In the sufficiently higher density the cage structure must give way to the IC triangular structure. Unfortunately we cannot calculate the energy of the IC phase under the periodic boundary condition; that is, we cannot predict the density of the cage-IC transition. However, it seems plausible to expect that the 15/36 cage structure is unstable, since the nearest atomic distance inside the cage is small as shown in Fig. 2. When even an excess ^{3}He atom was added to the 14/36 structure on a platelet of graphite, the cage structure would collapse into the IC structure simultaneously on the whole platelet or at least over a fairly large area. However, the collapse would not occur simultaneously on all platelets because of the finite distribution of the platelet size of Grafoil. That would occur at first on the largest platelet, then successively on the smaller. For the transitions on the smaller platelets, excess ^{3}He atoms must be added to the system. That is, the structural phase transition to the IC phase has a finite range of areal density, and the fraction of each structure does not change linearly with the density. The structural phase diagram at absolute zero temperature discussed here is schematically shown in Fig. 4. The transition between the HDW and the cage structures also takes place gradually due to the platelet size distribution. However, the range of transition is expected to be rather narrow. In Fig. 4 this range of transition is omitted for simplicity.

Here we examine the obtained phase diagram by comparison with experimental observations. GB observe kinks in the heat capacity isotherms at $T = 2.5$ and 5 mK at $\rho = 6.4$, 7.1, and 7.4 nm^{-2} [11]. These densities coincide with the boundaries of our phase diagram within the errors.
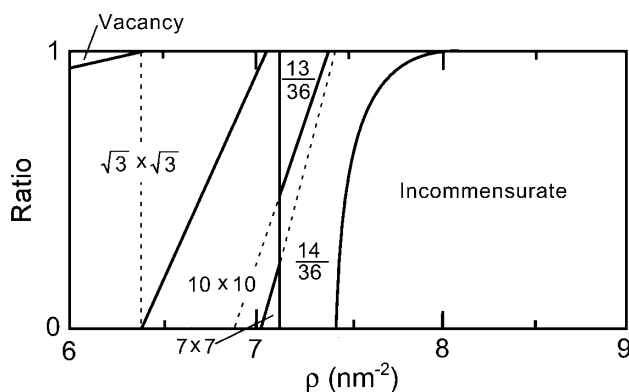

FIG. 4. The proposed phase diagram at absolute zero temperature. The vertical axis shows the proportion occupied by each structure. The coexistence of the $\sqrt{3} \times \sqrt{3}$ and 10×10 structures or of the honeycomb domain wall structures means the domain wall network structures or the striped structures.

The almost linear density dependence observed between kinks [11] is also in agreement with the supposed situation of the two-phase coexistence. GB observe weak kinks also at $\rho = 8.0$ nm^{-2} [11]. On some small platelets of graphite the 14/36 phase might survive up to the density of the 15/36 phase (7.95 nm^{-2}). These observed features in the isotherms should correspond to the change of the exchange frequencies. GB also observe a sudden jump at $\rho \approx 7.1$ nm^{-2} in the heat-capacity isotherm at $T = 200$ mK, which cannot be explained by the phase diagram proposed by them. In our phase diagram that is also explained as the sudden change of the Debye temperature due to the structural phase transition. In the measurements of the melting temperatures noticed with heat-capacity peaks by the Seattle group, sudden jump and kink are observed at $\rho \approx 7.1$ nm^{-2} and 7.5 nm^{-2}, respectively [13]. They also seem to correspond to the phase boundaries. These experimental observations support our proposed phase diagram.

Let us return to the problem of the MSE competition or of the features of α. Although we have not measured the heat capacity at 6.6 nm$^{-2} < \rho < 7.5$ nm^{-2}, α seems to decrease suddenly at $\rho \approx 7.5$ nm^{-2} (B). This behavior of α cannot be explained with GB's phase diagram assuming two-phase coexistence at this density [6,11]. Existence of a simple domain wall phase [12] also cannot explain that. In our phase diagram this density corresponds to the phase boundary of the commensurate (C)-IC transition. In the IC phase the effects of the potential corrugation must be weaker than in the cage phase, because the barrier due to the corrugation becomes shallower practically. Whether it strengthens or weakens the MSE competition is a delicate problem. Although the recent WKB calculation shows that the potential corrugation makes only the two- and three-spin exchanges relevant at the $\sqrt{3} \times \sqrt{3}$ phase [14], the observed sudden decrease of α indicates that the MSE competition is weaker in the IC phase in contrast to the case of the $\sqrt{3} \times \sqrt{3}$ phase. That is, the higher order MSEs become less important with the C-IC transition. Furthermore, in the IC phase the suppression of the MSEs by the corrugation must be much weaker than in the C phase. Considering also the predominance of the three-spin exchange over the two-spin exchange due to the rather high density, the sudden increase of J as the result of the C-IC transition seems a natural consequence. The phase boundary between the 14/36 and the IC phases schematically shown in Fig. 4 gives an abrupt and not linear increase of J with density. When the IC phase covers almost all the surface J must start to decrease. These arguments coincide with the experimental observations [4].

Figure 1 shows that the MSE competition varies even in the IC phase, especially the spike at $\rho \approx 8.5$ nm^{-2} (C) indicates the marked decline of the MSE competition. It is interesting that $\rho \approx 8.5$ nm^{-2} is very close to the density of the 4/9 structure, 8.49 nm^{-2}. The expected adsorption structure of the 4/9 is schematically shown in Fig. 5. One-fourth of the atoms (B atoms, dark grey colored) are
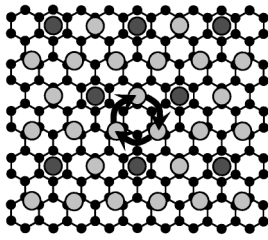
FIG. 5. The expected 4/9 adsorption structure of ^{3}He on graphite. For the three-spin exchange of bright grey colored circles (shown by arrows), the corrugation of the adsorption potential cannot be the barrier.

adsorbed on the most stable hollow site, while the rest (A atoms, bright grey colored) exist on the saddle point. For the three-spin exchange of A atoms the potential corrugation cannot be the barrier exceptionally. So the three-spin exchange dominates and higher order MSEs are negligible. That is why the normal behavior of C is observed at this density. Our path integral Monte Carlo simulation confirms that the structure shown in Fig. 5 is stable and the wave functions of ^{3}He atoms spread to the direction of the three-spin exchange tunneling path. Although in the magnetization measurement around $\rho = 8.5$ nm^{-2} no anomalous behavior was observed [4], precise density adjustment would be required.

Also in the second adsorbed layer of ^{3}He, similar cage structures based on the 4/7 structure [15] and the cage-IC structural phase transition could be expected. The transition is expected to occur between $7.39 < \rho_2 < 7.92$ nm^{-2} ($19.7 < \rho < 23.1$ nm^{-2}). Here ρ_2 is the second-layer areal density [16]. The upper and lower densities correspond to the 14/21 and 15/21 structures, respectively. The exchange frequency would start to increase with the appearance of the IC phase and become maximum when almost all the cage structure collapsed into the IC phase. This agrees with experimental observations [5,6]. The gradual decrease of α between $\rho = 7.3$ and 8.0 nm^{-2} [7] which shows similar behavior with $\ln\zeta$ [3] also agrees well with the argument that in the IC phase the MSE competition becomes weaker than in the C phase. That is, we can consider the same scenario with the submonolayer.

Our proposed hypothesis on the structure must be proved by systematic numerical calculation considering also dynamic adsorption structures. The direct observations by neutron diffraction experiments or by scanning microscopes, etc. are desirable. The theoretical calculation of the various exchange frequencies according to the present hypothesis with the potential corrugation will make clear the whole picture of the magnetism of adsorbed ^{3}He films.

To summarize, some specific features in density dependence of α, the exponent of heat capacities of ^{3}He submonolayer solid films adsorbed on Grafoil, are discussed. α is considered as the frustration parameter showing the strength of the MSE competition. We explain the fea-

tures by taking into account the evolution of the adsorption structure. For this purpose the structural phase diagram and the existence of zero-point vacancy are proposed. Our model can also explain qualitatively the appearance of the sudden ferromagnetic peak of the exchange frequency and other general aspects of many experimental observations. These facts support our interpretation that the exponent α reflects the strength of the MSE competition.

[1] H. Godfrin and H. J. Lauter, *Progress in Low Temperature Physics,* edited by W. P. Halperin (Elsevier, Amsterdam, 1995), Vol. XIV, p. 213.

[2] M. Roger, Phys. Rev. Lett. **64**, 297 (1990).

[3] M. Roger, C. Bäuerle, Yu. M. Bunkov, A.-S. Chen, and H. Godfrin, Phys. Rev. Lett. **80**, 1308 (1998); M. Roger, C. Bäuerle, and H. Godfrin, J. Low Temp. Phys. **113**, 249 (1998).

[4] H. Ikegami, K. Obara, D. Ito, and H. Ishimoto, Phys. Rev. Lett. **81**, 2478 (1998).

[5] H. Franco, R. E. Rapp, and H. Godfrin, Phys. Rev. Lett. **57**, 1161 (1986); H. Godfrin, R. R. Ruel, and D. D. Osheroff, Phys. Rev. Lett. **60**, 305 (1988); H. Godfrin, K.-D. Morhard, R. E. Rapp, and Yu. M. Bunkov, Physica (Amsterdam) **194B–196B**, 675 (1994).

[6] D. S. Greywall, Phys. Rev. B **41**, 1842 (1990).

[7] M. Morishita and H. Nagatani, and Hiroshi Fukuyama (to be published).

[8] Milton W. Cole, D. R. Frankl, and David L. Goodstein, Rev. Mod. Phys. **53**, 199 (1981).

[9] R. A. Guyer, Phys. Rev. Lett. **39**, 1091 (1977).

[10] R. Raghavan and V. Elser, Phys. Rev. Lett. **75**, 4083 (1995).

[11] D. S. Greywall and P. A. Busch, Phys. Rev. Lett. **65**, 2788 (1990).

[12] H. J. Lauter, H. Godfrin, V. L. P. Frank, and H. P. Schildberg, Physica (Amsterdam) **165B & 166B**, 597 (1990).

[13] M. Bretz, J. G. Dash, D. C. Hickernell, E. O. McLean, and O. E. Vilches, Phys. Rev. A **8**, 1589 (1973); S. V. Hering, S. W. Van Sciver, and O. E. Vilches, J. Low Temp. Phys. **25**, 793 (1976). Here their areal-density scale was shifted by several percent to make the maximum melting temperature coincide with the $\sqrt{3} \times \sqrt{3}$ solid.

[14] H. Ashizawa and D. S. Hirashima, Phys. Rev. B **62**, 9413 (2000).

[15] V. Elser, Phys. Rev. Lett. **62**, 2405 (1989).

[16] The conversion between the total density ρ and the second layer density ρ_2 is performed according to M. Roger, C. Bäuerle, H. Godfrin, L. Pricoupenko, and J. Treiner, J. Low Temp. Phys. **112**, 451 (1998).